Polymer Bulletin (2023) 80:9797–9810
https://doi.org/10.1007/s00289-022-04505-7

ORIGINAL PAPER

Preparation and evaluation of the antimicrobial activity of sodium alginate-grafted diphenylamine embedded with silver nanoparticles

Fatma Mohamed[1,2] · Asmaa Ahmed[2] · Omayma F. Abdel-Gawad[2]

Received: 11 March 2022 / Revised: 14 September 2022 / Accepted: 28 September 2022 /
Published online: 28 October 2022

Abstract

Antibiotic nanocomposite polymers show great promise in treating a variety of pathogens that cause widespread disease. Sodium alginate-grafted diphenylamine (NaAlg-g-DPA) embedded with different ratios of silver nanoparticles (AgNPs) was fabricated and characterized through different techniques including FTIR, XRD, and SEM techniques for investigating the antimicrobial activity. XRD confirmed the crystallinity of these compounds, and the average crystal size of Na Alg-g-DPA/Ag was estimated to be 48.6 nm. Then it was applied as an antimicrobial agent and evaluated through two ways (inhibition zone and MIC techniques) against *Staphylococcus aureus* as gram-positive bacteria with an inhibition zone of 19.31.6 mm and 18.60.63 mm against *Escherichia coli* as gram-negative bacteria while with increasing the Ag ratio 2:1 there was an enhancement in their biological activity to be 21.90.69 mm against *Staphylococcus aureus* and with an inhibition zone of 21.32.1 mm against *Escherichia coli*. The outcomes of this investigation are important for the development of new composite materials with antibacterial properties for industrial applications.

Keywords Sodium alginate · Diphenylamine · Silver nanoparticles · Antimicrobial activity

✉ Omayma F. Abdel-Gawad
omayma2013@hotmail.com

[1] Nanophotonics and Applications (NPA) Lab, Polymer Research Laboratory, Beni-Suef, Egypt

[2] Chemistry Department, Faculty of Science, Beni-Suef University, Beni-Suef 62514, Egypt

Introduction

One of the most significant issues that cause a threat to millions of people worldwide is microbial infection. *Staphylococcus aureus, Pseudomonas aeruginosa, Salmonella enteritidis*, and *Aspergillus niger* are the most pathogenic microorganisms that cause many diseases, including nausea, pneumonia, abdominal pain, enterocolitis, pyogenic liver abscess, hemorrhagic colitis, and diarrhea [1–6].

Consequently, many efforts were made to control this problem through developing new effective antimicrobial systems [7]. The development of antimicrobial resistance is considered the main target for antimicrobial drug delivery research. Biopolymer antimicrobials are the most widely used materials owing to their cost-effectiveness and ease of modification [8, 9].

Sodium alginate (biopolymer) is a group of naturally occurring anionic polysaccharides derived from brown seaweed and is generally considered biocompatible, non-immunogenic, and non-toxic polymers [10]. Alginates constitute a huge portion of the earth's organic matter because they are synthesized by living organisms such as plants, animals, bacteria, and fungi during their entire life cycle [11, 12]. Alginate has been grafted with different engineered polymers such as polyacrylamide (PAAm), polypyrrole (Ppy), and polydiphenylamineaniline (PDPA) to optimize the restriction of these synthetic polymers and improve their biodegradability and eco-friendly nature. The grafting of the manufactured polymer onto the biopolymer will improve the antimicrobial action against diverse species of organisms [13–16].

Polydiphenylamine (PDPA) is a significant polymer used as an antimicrobial agent for a long time due to the presence of nitrogen between two rings [17]. Diphenylamine derivatives have been shown to have a variety of biological activities, including anthelmintic activity (e.g., amoscanate [18]), analgesic and anti-inflammatory activity (e.g., diclofenac, tolfenamic acid [19]), and anticonvulsant activity (e.g., retigabine [20]).

In addition to the incorporation of different nanoparticles on polymer composite matrix are active functional hybrid materials containing nanoparticle and a polymer matrix. These materials have a wide range of beneficial uses in antimicrobial activity. The strengthened synergistic interaction between the constituent parts and the conductive network within the polymer matrix enhanced their activity.

Generally, one of the most popular materials for providing a variety of substrates with exceptional biological and mechanical properties is grafted polymer containing silver nanoparticles (AgNPs), which is also capable of resolving the common instability problem associated with the use of AgNPs-based coatings for fabrics after washing [21–26].

However, silver nanoparticles (Ag NPs) are most widely used in the evolution of new broad spectrum antimicrobial agents against pathogenic microorganisms. Silver nanoparticles are considered as potential therapeutic agents with a significant impact on respiratory medicine, via offering a multifunctional platform that could treat bacterial infections. They are synthesized by means of chemical reduction using highly reactive reducing agents [27, 28].

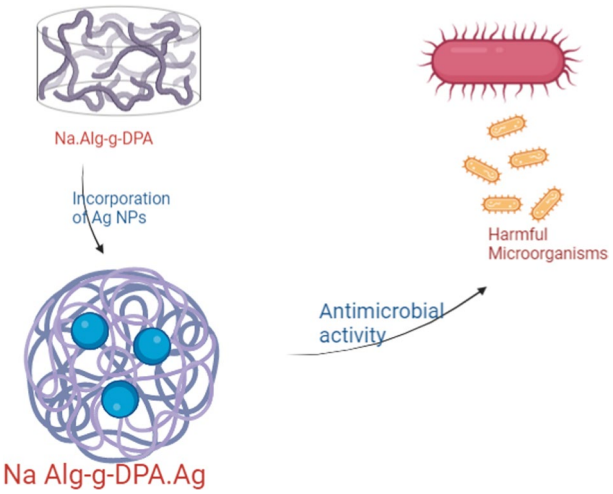

Fig. 1 Graphical abstract illustrated the antimicrobial activity of Na.Alg-g-DPA/Ag

AgNPs have piqued the interest of researchers due to their electronic properties, appealing optical properties, and excellent antimicrobial activities [29–31]. AgNPs have strong cytotoxicity for a wide range of microorganisms and are widely used as an antibacterial agent [32, 33].

Hence, the introduction of diphenylamine into sodium alginate also silver nanoparticles were embedded into the grafting substances to produce a new effective, safe, and cheap antimicrobial agent against various bacteria and fungi by a combination (Na.alg-g-DPA) with silver nano-particles with different concentrations of AgNPs of 1:1 and 1:2 AgNPs/Na.Alg-g-DPA ratio (Fig. 1). The new materials were characterized by FTIR, X-ray diffraction, and scanning and transmission electron microscopes. The new materials were tested against gram-positive strains (*Streptococcus pneumoniae ATCC 6*303 and *Staphylococcus aureus ATCC 29213*), gram-negative strains (*Pseudomonas aeruginosa ATCC 27853* and *Escherichia coli ATCC 25922*), and fungi (*Aspergillus fumigatus ATCC 13073* and *Candida albicans ATCC 10231*).

Materials and methods

Materials

Silver nitrate [TECHNO PHARMCHEM], glucose [Bio-chemical], polyvinyl pyrrolidine, sodium alginate, and ammonium persulfate were purchased from Sigma-Aldrich. Diphenylamine was purchased from Oxford Lab Chem. Hydrochloric acid and ethyl alcohol were purchased from Piochem.

Methods

Synthesis of NaAlg-g-DPA In flask (1), 25 ml of distilled water, 0.54 gm of sodium alginate (NaAlg), 2.1 gm of diphenylamine (DPA), and 1.9 ml of 1 M HCl were placed and stirred at 500 rpm for 1 h. In the flask (2), put 1 M of HCl (1.9 ml) and 0.5 M of Amm. per sulfite (APS) (2.85 gm) as an initiator in 25 ml of distilled water that was stirred at 500 rpm for 1 h. Flask (1) was slowly and carefully added to flask (2) under continuous stirring for 2 h. The system was kept for 24 h at room temperature. The solid product was separated by filtration and extracted by Soxhlet with distilled water and ethyl alcohol. The obtained solid was then dried for 24 h at 40 °C [34]. Soxhlet extraction is a method for controlling polymer solubility via a post-synthesis step. It is utilized for the extraction of a polymer from the impurities using a solvent in which the polymer is soluble.

Preparation of silver nanoparticles At three molar ratios, Ag:PVP is 1:1, 1:1.5, and 1:2. After dissolving 3.4 gm of silver nitrate ($AgNO_3$) in 20 ml of H^2O in beaker (A) and 10.2 gm of polyvinyl pyrrolidone (PVP) at a 1:1 ratio, 0.24 gm of NaOH, and 1.08 gm of glucose in 60 ml of H2O in beaker (B), the mixture was stirred continuously at 600 C, and the product was centrifuged several times. By repeating the steps for other ratios of Ag: PVP 1:1.5, 1:2 at the weight of PVP 15.3 gm, 20.4 gm, and Ag 3.4 gm.

PVP is crucial to the creation of silver NPs. It stops the created AgNPs from aggregating. The process through which PVP in an aqueous solution reduces silver ions to nanoparticles. Initially, a coordinative complex is created between silver ions and PVP by the donation of loan pair electrons from PVP's oxygen and nitrogen atoms to the silver's Sp orbitals. PVP encourages the nucleation of the metallic silver reduced by glucose in the second stage. Finally, PVP's steric action prevents the formation of silver grains and particles.

Preparation of sodium alginate-poly-diphenylamine silver nanoparticles (Fig. 2)

NaAlg-g-DPA/AgNPS weight ratios of 1:1 and 2:1 In Beaker (A), we put diphenylamine (DPA), synthesized AgNPs, Na-alginate, and HCL at 0.532 gm, 1.005 gm, 1.262 gm, and 0.87 ml, respectively, in 12 ml of H_2O, stirring for 1 h. In the beaker (B), put 0.87 ml of HCL and 1.166 gm of Amm. Persulfate (APS) and stirring for 1 h, then a beaker (B) was added to (A) dropwise. Finally, the mixture was stirred for 2 h. Finally, filter the product, wash it, and dry it very well.

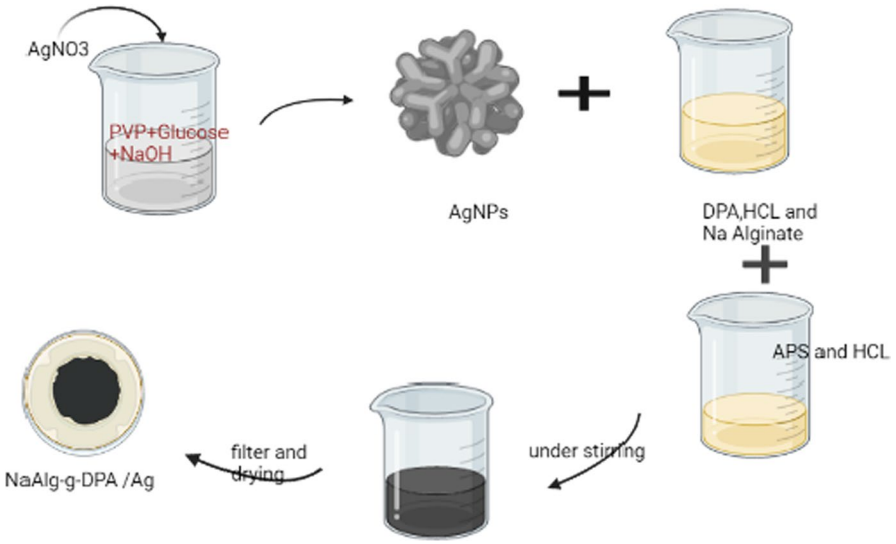

Fig. 2 Experimental part which illustrated the synthesis of NaAlg-g-DPA/AgNP

Instrumentations

Infrared spectroscopy

To confirm the occurrence of the reaction, using a Fourier transform infrared (FTIR) spectrometer (VERTEX 70 FT-IR). FT-IR spectra were recorded in ATR discs at room temperature within the wavenumber range of 4000–600 cm^{-1}.

X-ray diffraction

The crystalline structure of prepared copolymers was measured by X-ray diffraction (2020964 PA Analytical Empyrean), which is a technique that uniquely provides phase identification (e.g. graphite or diamond), along with phase crystallite size and quantification.

Scanning electron microscope

By using a scanning electron microscope (JEOL (JSM-5200)), the morphologies of the prepared copolymers were measured. Samples that prepared by placing a slight part of a film on a carbon tube on a stub, which was coated with a gold thin layer.

Results and discussion

Characterization

FTIR spectroscopy

Figure 3 shows the FTIR spectroscopy of AgNPs, Na.Alg-g-DPA and Na.Alg-g-DPA: AgNPs 2:1, respectively. All of the characteristic peaks for AgNPs/PVP are at 2923, 1460, and 1374 cm^{-1}, respectively. The peak at 1285–1295 cm^{-1}, typical for the C–N bond in PVP, was also presented. In AgNPs/PVP, a strong absorption peak, which is characteristic of the carbonyl group of PVP at 1650–1660 cm^{-1}, was observed. The peak was typical for the C–N bond at 1295 cm^{-1}. These peaks were associated with the formation of coordination bonds between silver atoms and oxygen or nitrogen atoms arising from PVP units [35]. In the Na.alg-g-DPA diagram in Fig. 3, the absorption peak at 3382 cm^{-1} corresponds to the O–H group, whose variations are shaped because of the contribution toward the reduction and stabilization processes. Other peaks appear at 1746, 1594, and 1501 cm^{-1}, which were attributed to the stretching vibration of the benzidine structure C = C and/or in C = N in the suggested polymer structure, while there are three strong absorption bands that appear at 745, 809, and 875 cm^{-1}, which were ascribed to out of plane C–H deformation showing 1,4-disubstitution in the benzene ring [36]. After incorporation of AgNPs into the grafting process, the peaks of 1501 and 1313 cm^{-1} shifted to 1485 and 1311 cm^{-1}, and 1029 cm^{-1}, indicating metal oxide nanomaterials, the hydroxyl groups, and carboxyl groups are shifted from 3382 and 1746 cm^{-1} to 3385 and 1741 cm^{-1}. The variations of the hydroxyl and carboxylate groups have been

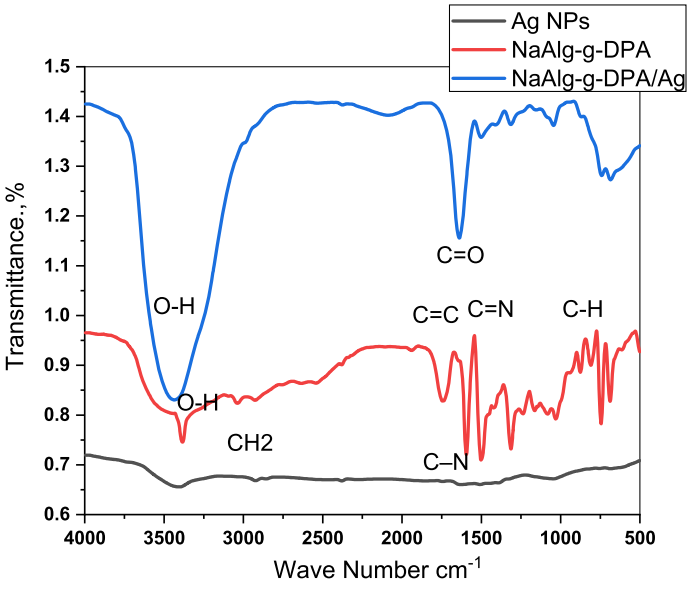

Fig. 3 FTIR for AgNPs, Na.Alg-g-DPA and NaAlg-g-DPA /Ag

reported in the previous study on the synthesis of AgNPs with another polysaccharide [37, 38].

XRD spectroscopy

Figure 4A–C shows the XRD patterns of AgNPs, NaAlg-g-DPA, and NaAlg-g-DPA/Ag, respectively. In the case of AgNPs (Fig. 4A), there are main peaks at 20.36°, 28.04°, 32.4°, and 38.3°, which appear in many works in which the XRD pattern includes the relevant 2 range. These peaks are due to the crystalline and amorphous organic phases accompanying crystallized AgNPs [39, 40]. The grafted sample (Fig. 4B) showed new diffraction peaks at 2 = 9.6°, 19.5°, 21°, and 28°, which related to DPA [41] that helped us in confirming the grafting process [42, 43]. As shown in Fig. 3C, the main peak corresponding to 100% appeared at 38.5°, while other peaks shifted to 47°, 65°, and 78°, indicating that the Ag NPs were spherical in structure and crystalline in nature [44]. The sharp peaks almost indicated some bioorganic compounds or proteins in the NPS

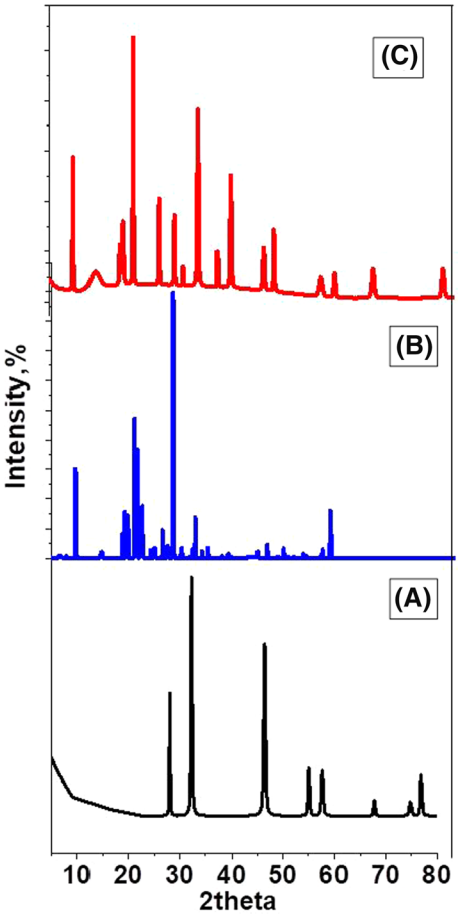

Fig. 4 X-ray diffraction (XRD) for **A** AgNPs, **B** NaAlg-g-DPA, **C** NaAlg-g-DPA/Ag

during synthesis [45]. These results prove the good incorporation of grafted polymer with Ag NPs. The average crystallite size (D) of Na.alg-g-DPA/Ag was calculated according to the Scherrer equation to be 48.6 nm.

Scanning electron microscopes

The scanning electron microscope (SEM) of NaAlg-g-DPA and NaAlg-g-DPA/Ag is shown in Fig. 5A–C. It was observed that sodium alginate's surface has been covered with a poly(DPA) grafted chain (Fig. 5A). A porous surface is produced by the ribose structure of grafted PDPA polymer on the sodium alginate surface. This novel surface structure is anticipated to enhance the antimicrobial activity of grafted polymer. After incorporation of AgNPs into the grafted polymer matrix, Fig. 5B, C shows small aggregates from AgNPs appeared on the surface of grafted Na.Alg-g-DPA. Additionally, the crystal size of the graft (Na.Alg-g-DPA) and AgNPs was 54.59 nm and 0.2 nm, respectively. The particle size was greater than the crystallite size obtained from XRD. This suggests that the apparent SEM particles may have consisted of more than one XRD crystallite. The AgNPs particles have a spherical shape stacked in regular shape, which proved the incorporation of AgNPs**.** The homogenous porous structure of NaAlg-g-DPA/Ag improves the antimicrobial activity of this compound [40].

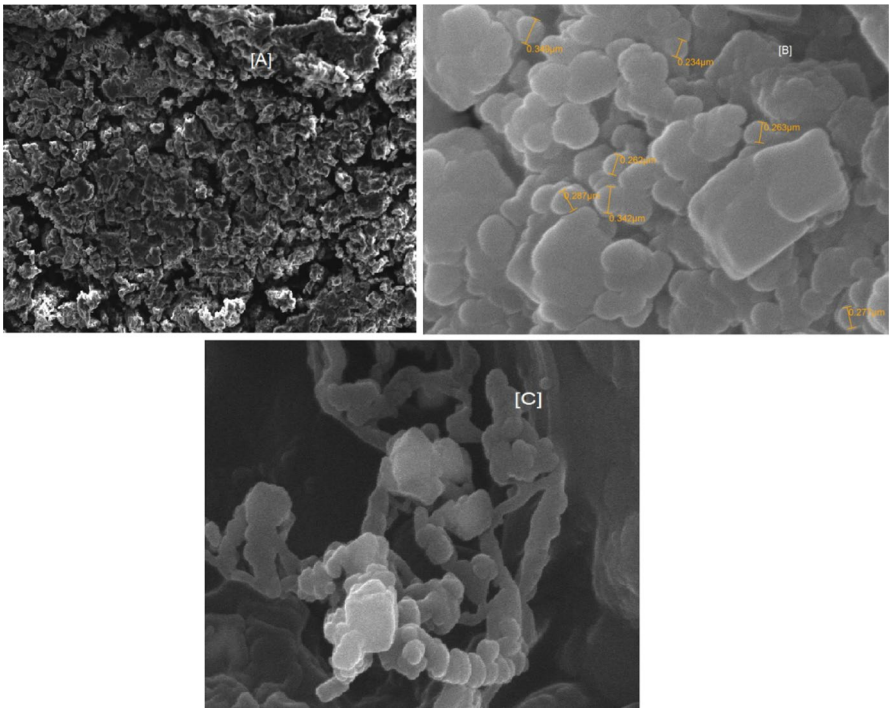

Fig. 5 SEM photography of **A** Na.alg-g-DPA, **B** and **C** Na.Alg-g-DPA/ Ag

Characterization by ^{1}H NMR

The ^{1}HNMR spectra of alginate and NaAlg-g-DPA are shown in Fig. 6. It was found that the backbone of alginate shows in obvious peaks at 4.0–4.5 ppm (Fig. 6a). In addition to NaAlg peaks, a new peaks appeared related to DPA δ7.25 (t, J = 7.0 Hz, 4H), 7.07 (d, J = 7.7 Hz, 4 H), 6.92 (t, J = 7.3 Hz, 2H) which confirm the successful grafting of DPA onto NaAlg successfully [33].

Antimicrobial activity

Nanotechnology's uses in the biomedical field have grown in recent years, with atomic-scale functional materials being used to fight and inhibit diseases. Two techniques (inhibition zone technique and minimum inhibitory concentration (MIC)) were used for antimicrobial evaluation of sodium alginate and the newly synthesized compounds (1–4). Different species of microbes were used for these tests, including *Streptococcus pneumoniae* (ATCC 6303), *Staphylococcus aureus* (ATCC 29213), as gram-positive bacteria, *Pseudomonas aeruginosa* (ATCC 27853), *Escherichia coli* (ATCC 25922) as gram-negative bacteria, and the antifungal activity against *Aspergillus fumigatus* (ATCC 13073), and *Candida albicans* (ATCC 10231). Tables 1 and 2 illustrate the inhibition zone diameter of the tested compounds against gram-positive and gram-negative bacteria and fungi.

Concerning sodium alginate (compound1), it has the lowest antimicrobial activity compared to the other synthesized compounds listed in Table 1, whereas the activity of grafted polymer was improved due to the presence of DPA chains, which may interact with the bacterial membrane via an electrostatic mechanism that causes a change in the potential gradient, which disrupts the cells [46].

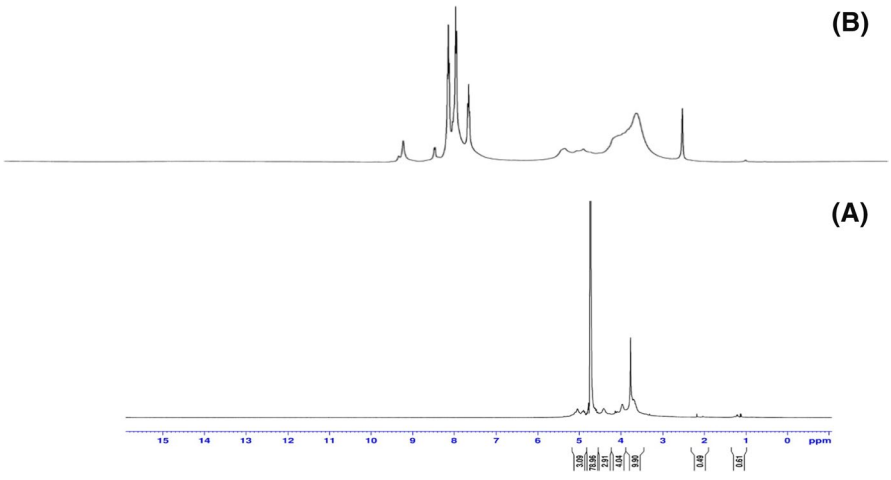

Fig. 6 Characterization by H-NMR spectroscopy for sodium alginate (**A**) and NaAlg-g-DPA (**B**)

Table 1 Mean zone of inhibition in mm ± Standard deviation beyond well diameter (6 mm) produced on a range of environmental and clinically pathogenic microorganisms

Tested microorganisms	Samples				
	Na.Alg (1)	Na.Alg-g-DPA (2)	Na.Alg-g-DPA: AgNPs 1–1 (3)	Na.Alg-g-DPA: AgNPs 2: 1 (4)	St
Fungi	Mean zone of inhibition (mm) ± Standard deviation				Amphotericin B
Aspergillus fumigatus ATCC 13073	10.3 ± 1.3	15.4 ± 1.3	19.5 ± 1.4	20.7 ± 1.4	21.9 ± 0.74
Candida albicans ATCC 10231	14.1 ± 0.82	18.2 ± 2.1	20.4 ± 1.6	21.8 ± 2.1	22.6 ± 1.9
Gram-positive Bacteria					*Ciprofloxacin*
Streptococcus pneumoniae ATCC 6303	16.3 ± 0.76	18.5 ± 0.58	20.6 ± 0.58	20.6 ± 0.85	22.1 ± 1.5
Staphylococcus aureus ATCC 29213	18.8 ± 0.98	19.3 ± 1.6	21.3 ± 2.1	21.9 ± 0.69	23.4 ± 1.2
Gram-negative Bacteria					*Ciprofloxacin*
Pseudomonas aeruginosa ATCC 27853	11.2 ± 1.3	17.4 ± 1.2	19.3 ± 1.3	19.4 ± 1.4	21.2 ± 0.76
Escherichia coli ATCC 25922	17.4 ± 2.1	18.6 ± 0.63	20.9 ± 1.5	21.3 ± 2.1	22.4 ± 1.3

However, the incorporation of AgNPs in grafted material (NaAlg-g-DPA/Ag) will enhance the antimicrobial activity and increased linearly with the ratios of AgNPs in the nanocomposites. AgNPs nanoparticles are potent candidates as antimicrobials owing t**o** their intrinsic properties and excellent thermal stability. These particles release silver ions which interact with bacterial cell walls causing breakage of the cell membrane [47].

The microbial activity significantly increased with the presence of AgNPs (compound3 with 1:1). Its inhibition zone was 18.50.58 and 19.31.6 mm against *Streptococcus pneumoniae* and *Staphylococcus* aureus as gram-positive bacteria, 17.41.2 and 18.60.63 mm against *Pseudomonas aeruginosa* and *Escherichia coli* as gram-negative bacteria, and 15.41.3 and 18.22.1 mm against *Aspergillus fumigatus* and *Candida albicans* as fungi, respectively.

The biological activity increases with increasing AgNPs ratios of 2: 1 (compound 4) to (20.60.85 and 21.90.69 mm against *Streptococcus pneumoniae* and *Staphylococcus aureus* as gram-positive bacteria, 19.41.4 and 21.32.1 mm against *Pseudomonas aeruginosa* and *Escherichia coli* as gram-negative bacteria, and 20.71.4 and 21.82.1 mm against *Aspergillus fum.*

Table 2 XTT assay detecting MICS (µg / ml) of tested samples against tested microorganisms

Tested microorganisms	Samples				
	Na.Alg(1)	Na.Alg-g-DPA (2)	Na.Alg-g-DPA: $AgNP_S$ 1:1 (3)	Na.Alg-g-DPA: AgNPs 2:1 (4)	St.
Fungi	Minimum inhibitory concentration (µg/ml)				Amphotericin B
Aspergillus Fumigatus ATCC 13073	250	62.5	3.9	1.95	0.98
Candida albicans ATCC 10231	62.5	7.81	1.95	0.98	0.49
Gram-positive bacteria					*Ciprofloxacin*
Streptococcus pneumoniae ATCC 6303	31.25	7.81	1.95	1.95	0.98
Staphylococcus aureus ATCC 29213	7.81	3.9	0.98	0.98	0.49
Gram-negative bacteria					*Ciprofloxacin*
Pseudomonas aeruginosa ATCC 27,853	125	15.63	3.9	3.9	1.95
Escherichia coli ATCC 25922	125	7.81	1.95	0.98	0.98

MIC is considered to be the significant standard technique to evaluate the susceptibility of a microorganism to a particular antibiotic and is performed as reported earlier [48, 49]. Table 2 represents the MIC values of the tested compounds (1–4) against the aforementioned organisms. These values are considered another evidence of the biological activity of the tested compounds, which also showed that NaAlg-g-DPA/Ag with a 2:1 ratio showed higher antibacterial and antifungal activity than others.

Conclusion

In this study, we were interested in new polymers containing different ratios of Ag NPs. The development of the novel class of composites depends crucially on their ability to resist different types of microbes. A new antimicrobial agent has been synthesized by grafting sodium alginate with diphenylamine and the incorporation of silver nanoparticles for evaluation against different types of bacteria and fungi using the agar diffusion method. The effect of the silver nanoparticle dopant ratio of the composite was studied in terms of antimicrobial activities. Pure grafted polymer showed a good antimicrobial effect with MIC 62.5, and increasing the content of Ag NPs doping significantly enhanced its performance against (gram-negative, gram-positive, and fungi) with MIC 3.9 and 0.98 for 1:1 and 2:1, respectively. These findings suggest that the DPA modified with Ag NPs has excellent scope for further

development as a commercial antimicrobial agent. Further experiments were needed to elucidate their mechanism of action.

Funding Open access funding provided by The Science, Technology & Innovation Funding Authority (STDF) in cooperation with The Egyptian Knowledge Bank (EKB).

References

1. Krishnaraj C, Ramachandran R, Mohan K, Kalaichelvan PT (2012) Optimization for rapid synthesis of silver nanoparticles and its effect on phytopathogenic fungi. Spectrochim Acta - Part A Mol Biomol Spectrosc 93:95–99. https://doi.org/10.1016/j.saa.2012.03.002
2. Wang H, Wang N, Wang B, Zhao Q, Fang H, Fu C et al (2016) Antibiotics in drinking water in Shanghai and their contribution to antibiotic exposure of school children. Environ Sci Technol 50:2692–2699. https://doi.org/10.1021/acs.est.5b05749
3. Wang G, Zhou S, Han X, Zhang L, Ding S, Li Y et al (2020) Occurrence, distribution, and source track of antibiotics and antibiotic resistance genes in the main rivers of Chongqing city, southwest China. J Hazard Mater 389:122110. https://doi.org/10.1016/j.jhazmat.2020.122110
4. Li F, Chen L, Chen W, Bao Y, Zheng Y, Huang B et al (2020) Antibiotics in coastal water and sediments of the East China Sea: distribution, ecological risk assessment and indicators screening. Mar Pollut Bull 151:110810. https://doi.org/10.1016/j.marpolbul.2019.110810
5. Elella MA, Abdel-Aziz* MM, Abd El-Ghany NA (2021) Synthesis of a high-performance antimicrobial o-quaternized alginate: a promising potential antimicrobial agent. Cellul Chem Technol 55(1–2):75–86
6. Abu-Thabit NY, Uwaezuoke OJ (2022) Superhydrophobic nanohybrid sponges for separation of oil/water mixtures. Chemosphere 294:133644
7. Langade CU (2019) Evaluation of antimicrobial activity of holopteliya integrifolia. Int J Sci Res 8:786–789
8. Goda ES, Elella MHA, Sohail M, Singu BS, Pandit B, El Shafey AM, Aboraia AM, Gamal H, Hong SE, Yoon KR (2021) N-methylene phosphonic acid chitosan/graphene sheets decorated with silver nanoparticles as green antimicrobial agents. Int J Biol Macromol 182:680–688
9. Pandit B, Goda ES, Abu Elella MH, ur Rehman A, Hong SE, Rondiya SR, Barkataki P, Shaikh SF, Al-Enizi AM, El-Bahy SM, Yoon KR (2022) One-pot hydrothermal preparation of hierarchical manganese oxide nanorods for high-performance symmetric supercapacitors. J Energy Chem 65:116–126
10. Sachan N, Pushkar S, Jha A, Bhattcharya A (2009) Sodium alginate: the wonder polymer for controlled drug delivery. J Pharm Res 2:1191–1199
11. Ngwuluka NC, Abu-Thabit NY, Uwaezuoke OJ, Erebor JO, Ilomuanya MO, Mohamed RR, Soliman SMA, Elella MHA, Ebrahim NAA (2021) Natural polymers in micro- and nanoencapsulation for therapeutic and diagnostic applications: Part II—polysaccharides and proteins. Nano- Microencapsul. https://doi.org/10.5772/intechopen.95402
12. Abu Elella MH, Hanna DH, Mohamed RR, Sabaa MW (2021) Synthesis of xanthan gum/trimethyl chitosan interpolyelectrolyte complex as pH-sensitive protein carrier. Polym Bull. https://doi.org/10.1007/s00289-021-03656-3

13. Abu Elella MH, Goda ES, Gab-Allah MA, Hong SE, Lijalem YG, Yoon KR (2022) Biodegradable polymeric nanocomposites for wastewater treatment. In: Advances in nanocomposite materials for environmental and energy harvesting applications, pp 245–298. doi:https://doi.org/10.1007/978-3-030-94319-6_9
14. Abu Elella MH, Goda ES, Gab-Allah MA, Hong SE, Pandit B, Lee S, Gamal H, Rehman A, Yoon KR (2020) Xanthan gum-derived materials for applications in environment and eco-friendly materials: a review. J Environ Chem Eng. https://doi.org/10.1016/j.jece.2020.104702
15. Abu-Elella MH, Goda* ES, Yoon KR, Hong SE, Morsy MS, Sadak RA, Gamal H (2021) Novel vapor polymerization for integrating flame retardant textile with multifunctional properties. Compos Commun 24: 100614
16. Abu Elella MH (2021) Synthesis and potential applications of modified Xanthan Gum. J Chem Eng Res Updates. https://doi.org/10.15377/2409-983X.2021.08.6
17. Kumar A, Mishra A (2015) Synthesis and antimicrobial activity of some new diphenylamine derivatives. J Pharm Bioallied Sci 7:81–85. https://doi.org/10.4103/0975-7406.148774
18. Franz M, Zahner H, Mehlhorn H, Striebel P (1990) Parasitnlngy 21833:393–400
19. Li Y, Qi X, Ming XX, Wu XF, Wu YF, Chen M et al (2009) The relationship between diphenylamine structure and NSAIDs-induced hepatocytes injury. Toxicol Lett 186:111–114. https://doi.org/10.1016/j.toxlet.2009.01.005
20. Douša M, Srbek J, Rádl S, Černý J, Klecán O, Havlíček J et al (2014) Identification, characterization, synthesis and HPLC quantification of new process-related impurities and degradation products in retigabine. J Pharm Biomed Anal 94:71–76. https://doi.org/10.1016/j.jpba.2014.01.042
21. Goda ES, Eissa AA-S, Pandit B, Abu-Elella MH (2022) Chalcogenides and phosphides for high-performance supercapacitors. Nanostruct Mater Supercapacitors. https://doi.org/10.1007/978-3-030-99302-3_19
22. Goda ES, Abu-Elella MH, Hong SE, Pandit B, Yoon KR (2021) Heba Gamal, smart flame retardant coating containing carboxymethyl chitosan nanoparticles decorated graphene for obtaining multifunctional textiles. Cellulose 28:5087–5105. https://doi.org/10.1007/s10570-021-03833-7
23. Abu-Elella MH, Goda ES, Abdallah HM, Elyamny S, Gamal H, Abu-Serea ES, Shalan AE (2022) Electroactive polymers for electrochromic applications. Electroactive Polymeric Materials, 1st Edition, (39)
24. Acik G, Altinkok C, Olmez H, Tasdelen MA (2018) Antibacterial film from chlorinated polypropylene via CuAAC click chemistry. Progr Organ Coat 125:73–78
25. Kalali EN, Guo W, Wang X, Xing W, Song L, Hu Y (2019) Effect of metal-based nanoparticles decorated graphene hybrids on flammability of epoxy nanocomposites. Compos: Part A 129:105694. https://doi.org/10.1016/j.compositesa.2019.105694
26. Abu-Elella MH, Sabaa MW, Hanna DH, Abdel-Aziz MM, Mohamed RR (2020) Antimicrobial pH-sensitive protein carrier based on modified xanthan gum. J Drug Deliv Sci Technol. https://doi.org/10.1016/j.jddst.2020.101673
27. Abdel-Aziz MM, Abu-Elella MH, Mohamed RR (2020) Green synthesis of quaternized chitosan/silver nanocomposites for targeting mycobacterium tuberculosis and lung carcinoma cells (A-549). Int J Biol Macromol. https://doi.org/10.1016/j.ijbiomac.2019.09.096
28. Abu-Elella MH, Goda ES, Abdallah HM, Shalan AE, Gamal H, Yoon KR (2021) Innovative bactericidal adsorbents containing modified xanthan gum/montmorillonite nanocomposites for wastewater treatment. Int J Biol Macromol 167:1113–1125. https://doi.org/10.1016/j.ijbiomac.2020.11.065
29. Wang H, Qiao X, Chen J, Ding S (2005) Preparation of silver nanoparticles by chemical reduction method. Colloids Surf A Physicochem Eng Asp 256:111–115. https://doi.org/10.1016/j.colsurfa.2004.12.058
30. Li D, He Q, Cui Y, Li J (2014) F of pH-responsive nanocomposites of gold, Nanoparticles/poly(4-vinylpyridine) CM 19 (2007) 412–417. Microwave-assisted synthesis of silver nanoparticles using sodium alginate and their antibacterial activity. Colloids Surf A Physicochem Eng Asp 444:180–188. https://doi.org/10.1016/j.colsurfa.2013.12.008
31. Jyothi A, Sashidhar RB, Arunachalam J (2010) Gum kondagogu (Cochlospermum gossypium): a template for the green synthesis and stabilization of silver nanoparticles with antibacterial application. Carbohydr Polym 82:670–679. https://doi.org/10.1016/j.carbpol.2010.05.034
32. Wei D, Qian W (2008) Facile synthesis of Ag and Au nanoparticles utilizing chitosan as a mediator agent. Colloids Surf B: Biointerfaces 62:136–142. https://doi.org/10.1016/j.colsurfb.2007.09.030

33. Ahmed A, Mohamed F, Elzanaty AM, Abdel-Gawad OF (2021) Synthesis and characterization of diphenylamine grafted onto sodium alginate for metal removal. Int J Biol Macromol 176:766–776. https://doi.org/10.1016/j.ijbiomac.2020.11.159
34. Ncube S, Lekoto G, Cukrowska E, Chimuka L (2018) Development and optimisation of a novel three-way extraction technique based on a combination of Soxhlet extraction, membrane assisted solvent extraction and a molecularly imprinted polymer using sludge polycyclic aromatic hydrocarbons as model compounds. J Sep Sci 41:918–928
35. Mohamed F, Bhnsawy N, Shaban M (2021) Reusability and stability of a novel ternary (Co–Cd–Fe)-LDH/PbI2 photoelectrocatalytst for solar hydrogen production. Sci Rep 11:5618
36. Bryaskova R, Pencheva D, Nikolov S, Kantardjiev T (2011) Synthesis and comparative study on the antimicrobial activity of hybrid materials based on silver nanoparticles (AgNps) stabilized by polyvinylpyrrolidone (PVP). J Chem Biol 4:185–191. https://doi.org/10.1007/s12154-011-0063-9
37. Fanta GF, Kenar JA, Felker FC, Byars JA (2013) Preparation of starch-stabilized silver nanoparticles from amylose-sodium palmitate inclusion complexes. Carbohydr Polym 92:260–268. https://doi.org/10.1016/j.carbpol.2012.09.016
38. Yang Z, Peng H, Wang W, Liu T (2010) Crystallization behavior of poly(ε-caprolactone)/layered double hydroxide nanocomposites. J Appl Polym Sci 116:2658–2667. https://doi.org/10.1002/app
39. Ponarulselvam S, Panneerselvam C, Murugan K, Aarthi N, Kalimuthu K, Thangamani S (2012) Synthesis of silver nanoparticles using leaves of Catharanthus roseus Linn. G. Don and their antiplasmodial activities. Asian Pac J Trop Biomed 2:574–580. https://doi.org/10.1016/S2221-1691(12)60100-2
40. Mohamed F, Enaiet Allah A, Abu Al-Ola KA, Shaban M (2021) Design and characterization of a novel ZnO–Ag/polypyrrole core–shell nanocomposite for water bioremediation. Nanomaterials 11:1688
41. Rajarajan K, Anandhi A, Reka KRD, Madhurambal G (2013) Synthesis and characterization studies of diphenylamine picrate cystal–a non-linear optical material. Interactions 9:10
42. Shaban M, Mohamed F, Abdallah S (2018) Production and characterization of superhydrophobic and antibacterial coated fabrics utilizing ZnO nanocatalyst. Sci Rep 8:1–15. https://doi.org/10.1038/s41598-018-22324-7
43. Mohamed F, Abukhadra MR, Shaban M (2018) Removal of safranin dye from water using polypyrrole nanofiber/Zn-Fe layered double hydroxide nanocomposite (Ppy NF/Zn-Fe LDH) of enhanced adsorption and photocatalytic properties. Sci Total Environ 640–641:352–363. https://doi.org/10.1016/j.scitotenv.2018.05.316
44. Kalaivani R, Maruthupandy M, Muneeswaran T, Hameedha Beevi A, Anand M, Ramakritinan CM et al (2018) Synthesis of chitosan mediated silver nanoparticles (Ag NPs) for potential antimicrobial applications. Front Lab Med 2:30–35. https://doi.org/10.1016/j.flm.2018.04.002
45. Shankar SS, Rai A, Ankamwar B, Singh A, Ahmad A, Sastry M (2004) Biological synthesis of triangular gold nanoprisms. Nat Mater 3:482–488. https://doi.org/10.1038/nmat1152
46. Kurowiak J, Kaczmarek-Pawelska A, Mackiewicz A, Baldy-Chudzik K, Mazurek-Popczyk J, Zaręba Ł, Klekiel T, Będziński R (2021) Synthesis, characterization and antimicrobial activity applications of grafted copolymer alginateg-poly(N-vinyl imidazole). RSC Adv 11:11541
47. Ehsan NK, Wenwen G, Xin W, Weiyi X, Lei S, Yuan H (2020) Effect of metal-based nanoparticles decorated graphene hybrids on flammability of epoxy nanocomposites. Compos Part A: Appl Sci Manuf 129:105694
48. Gokhan A, Cagatay A, Hulya OL, Mehmet AT (2018) Antibacterial film from chlorinated polypropylene via CuAAC click chemistry. Progr Organ Coat 125:73–78
49. Cagatay A, Gokhan A, Ozgun D, Hakan D, Ilknur T, Esra A (2022) A facile approach for the fabrication of antibacterial nanocomposites: a case study for AgNWs/poly(1,4-cyclohexanedimethylene acetylene dicarboxylate) composite networks by aza-Michael addition. Eur Polym J 169(15):111130